Photon Statistics of Semiconductor Microcavity Lasers

S. M. Ulrich,[1,*] C. Gies,[2] S. Ates,[1] J. Wiersig,[2] S. Reitzenstein,[3] C. Hofmann,[3] A. Löffler,[3] A. Forchel,[3] F. Jahnke,[2] and P. Michler[1]

[1]*Institut für Strahlenphysik, Universität Stuttgart, Germany*
[2]*Institut für Theoretische Physik, Universität Bremen, Germany*
[3]*Lehrstuhl für Technische Physik, Universität Würzburg, Germany*

(Received 2 March 2006; published 25 January 2007)

We present measurements of first- and second-order coherence of quantum-dot micropillar lasers together with a semiconductor laser theory. Our results show a broad threshold region for the observed high-β microcavities. The intensity jump is accompanied by both pronounced photon intensity fluctuations and strong coherence length changes. The investigations clearly visualize a smooth transition from spontaneous to predominantly stimulated emission which becomes harder to determine for high β. In our theory, a microscopic approach is used to incorporate the semiconductor nature of quantum dots. The results are in agreement with the experimental intensity traces and the photon statistics measurements.

DOI: 10.1103/PhysRevLett.98.043906 PACS numbers: 42.55.Sa, 42.50.Ar, 78.55.Cr, 78.67.Hc

In recent years, remarkable progress in semiconductor growth and processing has enabled the fabrication of tailored optical microresonators, which provide a high application potential in photonic devices, such as low-threshold microcavity lasers. Several types of solid-state microcavities [1], including micropillars [2,3], microdisks [4,5], and photonic crystals [6,7], offer very small mode volumes V_m in combination with high quality factors Q. In these structures, the number of optical modes is strongly reduced. As a consequence, the spontaneous emission (SE) coupling factor β of a mode, defined as the ratio of SE into that mode divided by the total SE into all modes, can become close to 1, with serious implications on the nature of light emission. With increasing β, the steplike "threshold" in the output intensity of conventional $\beta \ll 1$ laser devices gradually disappears up to the so-called thresholdless laser [8] in the limit $\beta = 1$.

According to earlier cavity QED approaches to the lasing dynamics in microresonators [9], a more accurate interpretation of the lasing onset and the nature of the emitted light is given by a photon statistics analysis. Based on a two-point counting statistics comparison between coincident (zero delay $\tau = 0$) and temporally uncorrelated (long delay) photon emission events, significant changes in the underlying field fluctuations from thermal to coherent behavior have been reported for microlasers with $\beta \sim 6 \times 10^{-3}$ [10].

Here we present comprehensive studies on the emission statistics and coherence properties of high-β micropillar lasers ($\beta = 0.04$ and 0.12) under both continuous (cw) and pulsed optical excitation. We use a quantum-dot (QD) ensemble as the active layer, which could provide an alternative gain medium to quantum wells as the conventional choice of present microlaser devices. Strong photon number fluctuations are identified from second-order correlation measurements, revealing "bunching" within a smooth transition to coherent light emission. The measurements are compared to results of a microscopic theory for the coupled light-matter dynamics to describe the threshold behavior of the QD micropillars. This new theory is capable of accounting for semiconductor effects that render QDs different from atoms [11,12].

The micropillars are grown by molecular beam epitaxy on a (001)-GaAs substrate, with a high-reflection planar cavity structure consisting of 27 (23) bottom (top) distributed Bragg reflector (DBR) periods of alternating AlAs (76 nm)/GaAs (66 nm) $\lambda/4$ layer pairs. Two 130 nm GaAs spacer layers between the DBR stacks form a λ cavity, centered around a single layer ($d = 4.5$ nm) of self-assembled $In_{0.30}Ga_{0.70}As$ QDs (density of $\sim 6 \times 10^9\,cm^{-2}$). Combined e^--beam lithography and plasma-induced reactive ion etching were used to process high quality arrays of cylindrically shaped micropillar structures [13]. The measurements of this Letter were performed on two selected 3 and 4 μm diameter pillars. A scanning electron microscope (SEM) side view of a 3 μm pillar is shown in Fig. 1(a), demonstrating an almost per-

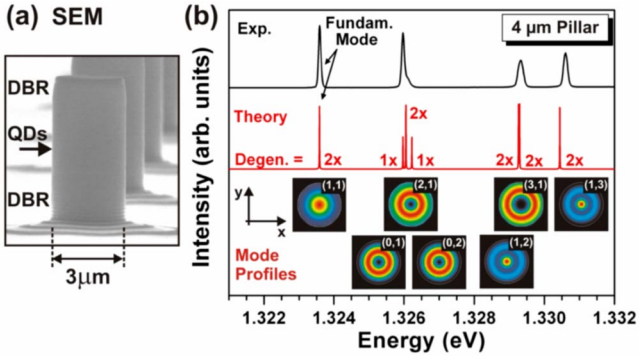

FIG. 1 (color online). (a) SEM image of a 3 μm micropillar. (b) Experimental (top)/theoretical (bottom) verification of the pillar mode spectra ($1\times$, $2\times$ mode degeneracy) for the 4 μm structure. Inset: Calculated transverse mode profiles with radial/angular quantum numbers (m, l).

fect structural shape together with a smooth surface texture.

All studies on the micropillar emission characteristics have been performed on a combined low-temperature ($T = 4$ K) microphotoluminescence (μPL) and a Hanbury Brown–Twiss (HBT) second-order photon-correlation setup [14]. For experiments under pulsed nonresonant excitation above the GaAs barrier ($E_g^{4K} = 1.52$ eV [15]), a mode-locked Ti:sapphire laser tuned to 800 ± 1 nm and providing $\Delta t_{\mathrm{las}} \approx 150$ fs or 1.4 ps wide pulses at $f_{\mathrm{exc}} = 82(76)$ MHz was used. Micro-PL and $g^{(2)}(\tau)$ correlation experiments under cw pumping were performed by a Ti:sa ring laser operated at 800 nm. A 1 m double monochromator with a ℓN-cooled CCD (resolution $\Delta E \approx 30$ μeV) was used for spectral imaging and filtering. All photon-correlation measurements have been recorded by avalanche photodiodes (AQR-14) in multichannel coincidence counting, with an instrumental accuracy (IRF) of $\Delta t_{\mathrm{IRF}} \approx 600$ ps. Additional first-order $g^{(1)}(\tau)$ coherence measurements on the spectrally filtered pillar mode emission were performed on a computer-controlled Michelson interferometer.

To reveal the optical mode structure of the micropillars, the inhomogeneously broadened emission of the QD ensemble is used as a cavity-internal light source. As shown for the 4 μm structure in Fig. 1(b) (top), a series of narrow emission modes is observable. These eigenmodes have been identified from calculations on the basis of an extended transfer matrix method [16]. Excellent agreement is found from a direct comparison [Fig. 1(b)]. The mode degeneracies together with their transverse (cross-sectional) intensity patterns are depicted below.

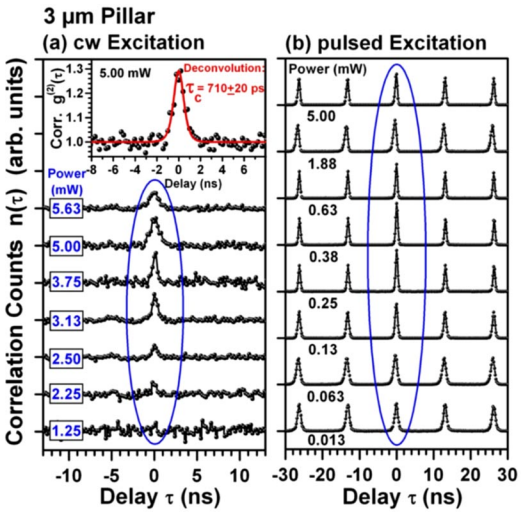

FIG. 2 (color online). (a) $\tilde{g}^{(2)}(\tau)$ correlation series for the 3 μm fundamental pillar mode under varying cw excitation, clearly revealing photon bunching $\tilde{g}^{(2)}(0) > 1$. Inset: Coherence time fit to the 5.0 mW trace under convolution with the temporal IRF ($\Delta t_{\mathrm{IRF}} \approx 600$ ps). (b) Power-dependent autocorrelation series of the same micropillar under pulsed excitation, again reflecting a strong bunching effect at $\tau = 0$.

From the spectral emission widths at low excitation, quality factors of $Q_{\mathrm{exp}} \approx E/\Delta E = 8600 \pm 300$ (3 μm) and $12\,300 \pm 500$ (4 μm) have been estimated for the fundamental modes [$\sim$1.3346 eV (3 μm) and $\sim$1.3234 eV (4 μm)].

Figures 2(a) and 2(b) depict photon-correlation results from the 3 μm pillar's fundamental mode emission under cw and pulsed excitation, respectively. In the pulsed experiments, the effect of bunching is clearly observable, reflected as an increase of the center ($\tau \approx 0$) with respect to neighboring correlation peaks at $\tau = n\Delta t_{\mathrm{exc}} = n/f_{\mathrm{exc}}$ within a broadened excitation power range around the stimulated emission onset. Autocorrelation measurements under cw excitation also reveal a strongly enhanced two-photon coincidence probability at short delays $|\tau| \leq \tau_c$ (τ_c: coherence time) for intermediate powers. For a correct description of the experimental correlation traces $\tilde{g}^{(2)}(\tau)$ under consideration of the HBT temporal resolution Δt_{IRF}, a fit function as a convolution of the idealized expression $g^{(2)}(\tau) = 1 + b_0 \exp(-2|\tau|/\tau_c)$ (b_0: bunching amplitude) with a Gaussian function of width $2\sigma = \Delta t_{\mathrm{IRF}}$ has been applied as

$$\tilde{g}^{(2)}(\tau) = 1/\sqrt{2\pi\sigma^2} \int_{-\infty}^{\infty} d\tau' g^{(2)}(\tau - \tau') \exp(-\tau'^2/2\sigma^2). \quad (1)$$

From fits to the normalized cw $\tilde{g}^{(2)}(\tau)$ traces, coherence times of 710 ± 20 ps [$P_0^{\mathrm{cw}} = 5$ mW; inset in Fig. 2(a)] and 480 ± 30 ps (4.375 mW; not shown) have been evaluated. As is demonstrated below, these values reveal excellent agreement with direct measures of the coherence times.

In the bottom parts of Figs. 3(a) and 3(b), the fundamental mode intensity traces of the 3 (4 μm) pillar samples under pulsed excitation are shown. In either case, an s-shaped smooth intensity transition [17,18] appears at

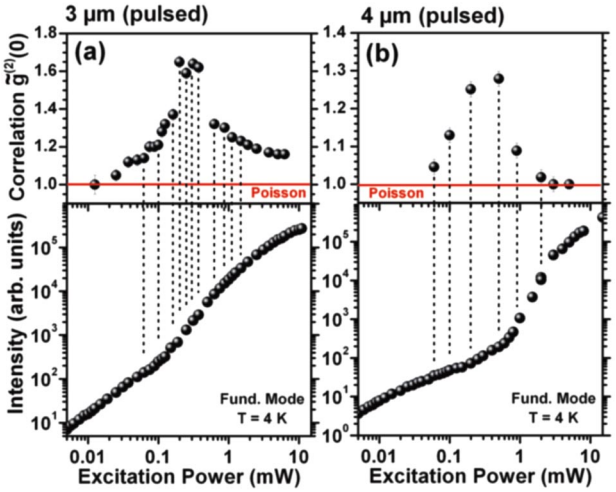

FIG. 3 (color online). (a),(b) Integrated intensities (bottom) for the 3 (4 μm) pillars under nonresonant pulsed excitation. Strong photon bunching $\tilde{g}^{(2)}(0) > 1$ is found from corresponding correlation measurements (top) over a broadened regime around the threshold.

intermediate excitation levels of ~200 (~500 μW) for the 3 (4 μm) pillar, respectively. As is exemplarily depicted in Fig. 4(b) for the 3 μm pillar, an equivalent trend is also found in the cw intensity traces, where the *s*-shaped threshold region is not fully developed due to experimental limitations.

In Figs. 3(a), 3(b), 4(a), and 4(b), indications of strong photon field fluctuations are consistently observed over the full onset regions (~ $\pm$1 decade) of stimulated emission in all traces of $\tilde{g}^{(2)}(0)$. In the regime well below the threshold, the measured $\tau = 0$ correlations remain close to 1, in contrast to an expected thermal behavior with $g^{(2)}(0) > 1$ [9]. In order to clarify this observation, supplemental cw power-dependent $g^{(1)}(\tau)$ first-order field correlation measurements by Michelson interferometry have been performed on the same 3 μm pillar. As is shown in Fig. 4(c), a strong decrease of the coherence time τ_c from 700 down to <50 ps is directly monitored within the nonlinear transition region. We therefore attribute the observed $\tilde{g}^{(2)}(0) \rightarrow 1$ decrease at low excitation powers to the temporal detection limits of the HBT setup (Δt_{IRF}), which no longer resolve the "real" $g^{(2)}(\tau = 0)$ result but represent a convolution over extended time scales $\tau \gg \tau_c$ with $g^{(2)}(\tau > \tau_c) \approx 1$. This is also demonstrated in the theory section. Moreover, our experiment-theory investigations comply with recent data on high-β photonic crystal lasers [19] showing such $\tilde{g}^{(2)}$ characteristics around the lasing onset.

As also becomes obvious from Fig. 3, the Poisson limit of $\tilde{g}^{(2)}(0) = 1$, denoting stabilized coherent emission, is only gradually approached. Noticeable bunching signatures are still observable at excitation levels of >10× (5×) increased excitation powers above the transition onsets into stimulated emission (3 μm: ~200 μW; 4 μm: ~500 μW).

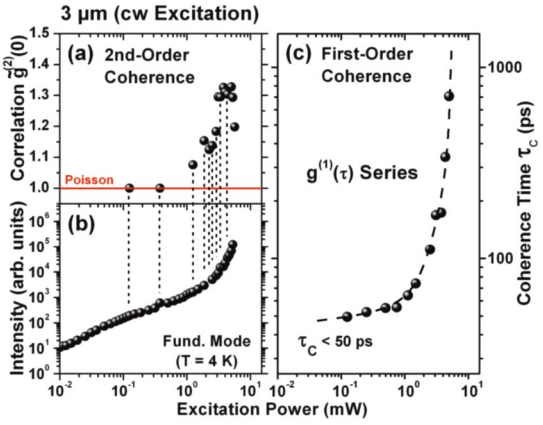

FIG. 4 (color online). (a) $\tilde{g}^{(2)}(\tau = 0)$ autocorrelation results derived from the 3 μm pillar fundamental mode under cw excitation [see series in Fig. 2(a)], together with the corresponding mode emission intensity (b). (c) First-order $g^{(1)}(\tau)$ series, revealing a strong τ_c coherence decrease in the low excitation limit.

In the past, theoretical models of photon correlations have been based on atomic systems. Recently, differences between the emission properties of QDs and atoms have been discussed [11,12]. In semiconductors, recombination processes require the presence of both electrons and holes, which are not necessarily fully correlated. Scattering processes can redistribute electrons and holes independently, and dephasing as well as screening effects can reduce (excitonic) electron-hole correlations due to Coulomb interaction. Only the fully correlated case corresponds to the atomic picture. From the semiconductor Hamiltonian for the interacting carrier-photon system, we determine the time evolution of the carrier population and the photon number using Heisenberg's equations of motion. In order to truncate the arising equation hierarchy, we use the cluster expansion [20] which was previously applied to describe the luminescence dynamics of quantum wells [21] and QDs [11,12]. In this Letter, we address intensity fluctuations, which are discussed in terms of the second-order correlation $g^{(2)}(\tau = 0) = (\langle n^2 \rangle - \langle n \rangle)/\langle n \rangle^2$. Here $n = b^\dagger b$ is the photon number operator, expressed via creation and annihilation operators for the laser mode. The autocorrelation function can be written in terms of the correlation function $\delta\langle b^\dagger b^\dagger bb \rangle = \langle b^\dagger b^\dagger bb \rangle - 2\langle b^\dagger b \rangle^2$, being fourth-order in the cluster expansion: $g^{(2)}(0) = 2 + \delta\langle b^\dagger b^\dagger bb \rangle / \langle b^\dagger b \rangle^2$. For a self-consistent theory on this level, we start with equations of motion for the photon number and the electron and hole populations, $f_\nu^e = \langle c_\nu^\dagger c_\nu \rangle$ and $f_\nu^h = 1 - \langle v_\nu^\dagger v_\nu \rangle$, where ν is the carrier operators' electronic state index. The source term of these equations contains the photon-assisted polarization $\langle b^\dagger v_\nu^\dagger c_\nu \rangle$, which introduces the additional carrier-photon correlations $\delta\langle b^\dagger b c_\nu^\dagger c_\nu \rangle$ and $\delta\langle b^\dagger b v_\nu^\dagger v_\nu \rangle$. Their dynamics, as well as the equation of motion for $\delta\langle b^\dagger b^\dagger bb \rangle$, are

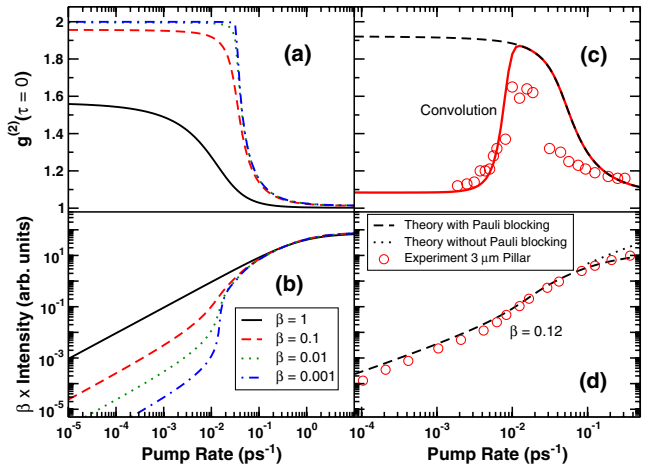

FIG. 5 (color online). (a),(b) Calculated output curves (bottom) and $g^{(2)}(0)$ (top) for various β. (c),(d) Calculated results vs experimental data (pulsed) from Fig. 3(a) for the 3 μm pillar. In (c), a convolution (solid line) with the experimental temporal resolution τ_c is shown. (d) Corresponding I/O curves, explicitly indicating the effects of pump saturation.

coupled to the dynamics of $\delta\langle b^\dagger b^\dagger b v_\nu^\dagger c_\nu\rangle$. For a basic explanation of our experimental observations, Coulomb effects are restricted to renormalized interband couplings, effective transition energies, and scattering rates.

For the calculations, we distinguish between the laser mode and nonlasing modes. The equation of motion for the photon-assisted polarization of the nonlasing modes is eliminated adiabatically in order to introduce the β factor. We consider QDs with two confined shells, with the laser transition between the s shells. The pump process is modeled with a constant carrier generation rate into the p shell, incorporating saturation effects due to Pauli blocking. We consider fast carrier scattering from the p to the s shell in relaxation time approximation [22]. Rates for cavity losses and damping of polarizationlike correlations are also introduced.

Figures 5(a) and 5(b) show results for various values of β. We use $\tau_{\mathrm{sp}} = 27$ ps for the total SE time and $\tau_{\mathrm{cav}} = 13$ ps for the cavity lifetime. Here the number of QDs is increased with decreasing β to compensate the reduced emission into the laser mode. In the logarithmic representation in Fig. 5(b), the s-shaped intensity jump is found not to scale with β^{-1}—in contrast to the predictions of rate equations [9]. This is a direct result of our semiconductor model with a modified source term of SE and the absence of complete population inversion. In the limit $\beta = 1$, no kink is visible, reflecting all stimulated and spontaneous emission to be coupled to the laser mode.

The calculated true correlation function $g^{(2)}(\tau = 0)$ is shown in Fig. 5(a), revealing the value of 2 for thermal light below the threshold and $\beta \ll 1$. In the threshold region, the correlation function decreases to unity, as the expected value for coherent laser light. For large values of β, this transition becomes broader while still indicating the onset of coherent emission, and $g^{(2)}(0)$ deviates from 2 below threshold. This reduction is a consequence of a large Q factor, a small number of emitters, and a fast SE rate and is therefore a characteristic of high-Q microcavity lasers. In the theoretical limit $Q \to \infty$, $g^{(2)}(0)$ is always 1 [9].

Figure 5(d) provides a comparison of the calculations for the pulsed measurements of the 3 μm pillar with $\tau_{\mathrm{cav}} = 13$ ps, a SE time into the laser mode of $\tau_{\mathrm{lase}} = 250$ ps, and 42 resonant QDs, yielding $\beta = 0.12$, in good agreement with the observed intensity trace. Saturation effects become visible in the high excitation regime, indicative of blocking of the rapidly filled pump levels. Similarly, $\beta = 0.04$ reproduces the 4 μm pillar results (not shown).

Figure 5(c) depicts the calculated autocorrelation function. For a direct comparison with our $\tilde{g}^{(2)}$ experiments (limited by Δt_{IRF}), we have adapted the measured coherence times τ_c to our results in Figs. 5(c) and 5(d). Since the upper output intensity branch is not accessible for cw pumping, this can be done only qualitatively. We determine $g^{(2)}(\tau)$ for each pump intensity from the calculated $g^{(2)}(0)$ via $g^{(2)}(\tau) = 1 + [g^{(2)}(0) - 1]\exp(-2|\tau|/\tau_c)$ and convolve with an apparatus function as discussed in the first section [Eq. (1)]. The $\tau = 0$ value of this convolution is shown as a solid line in Fig. 5(c), reproducing the measured $\tilde{g}^{(2)}(0)$ correlation "peak" and its incomplete decay into full coherence, the latter being caused by saturation effects.

In summary, the emission properties of quantum-dot based microcavity lasers with large spontaneous emission coupling have been studied. In this regime, the statistical properties of the light emission are analyzed by photon-correlation measurements. A smooth transition from spontaneous emission with strong photon bunching to stimulated emission with a Poissonian statistics is observed. Our results are in good agreement with calculations of the intensity and intensity fluctuations based on a novel semiconductor theory.

We gratefully acknowledge financial support from the DFG research group "Quantum optics in semiconductors" and the Alexander-von-Humboldt Foundation, as well as a grant for CPU time at the Forschungszentrum Jülich (Germany).

*Corresponding author.
Electronic address: s.ulrich@physik.uni-stuttgart.de

[1] J.-M. Gérard, in *Single Quantum Dots—Fundamentals, Applications and New Concepts*, edited by P. Michler, Topics in Applied Physics Vol. 90 (Springer, New York, 2003), Chap. 7; K. J. Vahala, Nature (London) **424**, 839 (2003), and references therein.
[2] M. Pelton *et al.*, Phys. Rev. Lett. **89**, 233602 (2002).
[3] J. P. Reithmaier *et al.*, Nature (London) **432**, 197 (2004).
[4] P. Michler *et al.*, Science **290**, 2282 (2000).
[5] E. Peter *et al.*, Phys. Rev. Lett. **95**, 067401 (2005).
[6] T. Yoshi *et al.*, Nature (London) **432**, 200 (2004).
[7] A. Badolato *et al.*, Science **308**, 1158 (2005).
[8] F. De Martini and G. R. Jacobovitz, Phys. Rev. Lett. **60**, 1711 (1988).
[9] P. R. Rice and H. J. Carmichael, Phys. Rev. A **50**, 4318 (1994).
[10] R. Jin *et al.*, Phys. Rev. A **49**, 4038 (1994).
[11] M. Schwab *et al.*, Phys. Rev. B **74**, 045323 (2006).
[12] N. Baer *et al.*, Eur. Phys. J. B **50**, 411 (2006).
[13] A. Löffler *et al.*, Appl. Phys. Lett. **86**, 111105 (2005).
[14] R. Hanbury Brown and R. Q. Twiss, Nature (London) **177**, 27 (1956).
[15] *Numerical Data and Functional Relationship in Science and Technology*, edited by K.-H. Hellwege and O. Madelung, Landolt-Börnstein, New Series, Group III, Vol. 17a (Springer, Berlin 1982).
[16] D. Burak and R. Binder, IEEE J. Quantum Electron. **33**, 1205 (1997).
[17] J. Hendrickson *et al.*, Phys. Rev. B **72**, 193303 (2005).
[18] S. Reitzenstein *et al.*, Appl. Phys. Lett. **89**, 051107 (2006).
[19] S. Strauf *et al.*, Phys. Rev. Lett. **96**, 127404 (2006).
[20] J. Fricke, Ann. Phys. (N.Y.) **252**, 479 (1996).
[21] W. Hoyer, M. Kira, and S. W. Koch, Phys. Rev. B **67**, 155113 (2003).
[22] T. R. Nielsen, P. Gartner, and F. Jahnke, Phys. Rev. B **69**, 235314 (2004).